INVESTIGATING DAMAGE RESISTANCE OF HYBRID COMPOSITE-METALLIC STRUCTURES USING MULTI-SCALE COMPUTED TOMOGRAPHY

T. Allen[a*], A. E. Scott[a], W. Hepples[b], S. M. Spearing[a], P. A. Reed[a], I. Sinclair[a],

[a]*Engineering Materials, Faculty of Engineering and the Environment, University of Southampton, University road, Southampton, SO17 1BJ, United Kingdom*
[b]*Luxfer Gas Cylinders, Colwick, Nottingham, NG4 2BH, United Kingdom*
**tma1e12@soton.ac.uk*

Keywords: Computed Tomography, Non-Destructive Testing, Impact, Damage Resistance

Abstract
In this work multi-scale computed tomography (CT) is used to investigate the effect of an industrial low velocity impact protocol on hybrid composite-metallic structures (HCMS). The results show the complex impact response of HCMS to be a combination of fibre fracture, intra-laminar cracks, delamination and plastic deformation of the metallic component. After the initial post-impact CT scanning the structure was subjected to a single load cycle and rescanned. Sub-micron resolution local CT scans revealed no evidence of fibre fracture within the scanned regions of interest.

1. Introduction

Hybrid composite-metallic structures (HCMS) are used in a variety of industrial applications where strength, stiffness and weight are important properties. In certain applications dynamic loading events, such as low-velocity impacts (LVI), are inevitable from both foreign object impact and handling mishaps. Fully understanding LVI events and the underlying failure mechanisms that control post-impact performance is essential to improve HCMS design.

The impact response of similar HCMS has been investigated experimentally previously [1-4]. However, previous HCMS impact studies have relied largely on surface based inspection or destructive damage assessment techniques through sectioning and microscopy. Scott *et al.* [5] used a multi-scale computed tomography approach to investigate damage progression non-destructively in HCMS when subject to uniform internal loading. Multi-scale CT has also been used as a tool for investigating impact on carbon fibre reinforced plastic (CFRP) [6]. This research utilises a multi-scale CT approach to assess the impact response of HCMS, providing a novel visualisation of the impact response and post-impact performance of HCMS.

2. Materials and method

2.1. Materials
The HCMS structure investigated was specially manufactured for the experimental study. It is made of an aluminium alloy hoop structure, over-wrapped with CFRP and glass fibre reinforced plastic (GFRP). The CFRP and GFRP layers were filament wound on to the

aluminium shell, creating a structure of 160mm OD and 525mm in length. The thicknesses of the aluminium, CFRP and GFRP are 2.5mm, 4.5mm and 1mm respectively. The CFRP has four plies, two circumferentially wrapped plies and two large angle longitudinal layers.

2.2 Method

No previous work has been found in the open literature in which µCT has been used to visualise impact events on HCMS. The LVI event was of 120J impact energy with a metal edge impactor.

The sample was CT scanned directly after impact and then subjected to a single uniform load cycle of 30MPa. The sample was then cut into small “matchstick” sections in order to achieve higher resolution CT scans of regions of interest (ROI) at a “meso-” and micro-structural level. This was in order to interrogate the material response to the impact and to gain more insight into the residual properties of the CFRP layer, which contributes the majority of the strength and stiffness to the HCMS.

2.3 CT Scanning

Scans at three length scales are presented in this work:

- Macro-structure: global impact site scans using µCT (~30mm wide field of view (FOV))
- Meso-structure: ply level scans of matchstick samples prepared from the sample (~4mm wide FOV)
- Micro-structure: local sub-region scans of matchstick samples to achieve a sub-micron resolution capable to resolve individual carbon fibres (~1mm FOV)

The macro-structure scan was completed on a custom-built Nikon Metrology µCT scanner at the µ-VIS centre at the University of Southampton. The scanner has a 225kV X-ray source and Perkin-Elmer 1621 2048 x 2048 pixel flat panel detector. An electron accelerating voltage of 180kV was selected, with a tungsten reflection target and a beam current of 145µA. 3142 projections were taken during the 360º rotation of the sample, four frames taken per projection with a 1 second exposure time. A 1mm copper filter was used. 3D reconstruction with a voxel size of 23.7µm was created using filtered-back projection within the Nikon CT Pro 2.0 package. Image processing and analysis was completed using the software packages ImageJ and VGStudio max 2.1.

The meso and microstructure scans were completed on a standard Xradia Versa 510, a lab based CT machine capable of achieving 700nm resolution. The scanner has a 160kV transmission source with a tungsten target. A detector system similar to synchrotron radiation CT station is used, employing a scintillator and optical microscope optics, with a 2048 x 2048 pixel field of view. The meso-structure scans achieved a voxel size of 4.6µm, using scan settings of 60kV and 5W with a 1 second exposure time, 2X binning (whereby 4 adjacent pixels are combined into one, to improve signal-to-noise) and a 4X objective. 1601 projections were taken during the 360º rotation of the sample. The microstructure CT scans achieved a voxel size of 0.96µm, using scan settings of 70kV and 7W with 1 second exposure time, 2X binning and a 4X objective. 3201 projections were taken during the 360º rotation of the sample.

3. Results

3.1 Macro-structure CT results

The scan of the impact site revealed substantial subsurface damage (Figure 1, Figure 2). A 3D visualisation of the impact site is presented in Figure 3. Several damage mechanisms are present in the CFRP layer. It is also clear from the scan data that plastic deformation of the metal layer has occurred. The maximum depth of this dent measured 0.75mm (Figure 2).

As mentioned previously the scan data has a voxel size of ~24µm, the carbon fibres have a diameter of ~7µm. This means it is not possible to quantify individual fibre breaks at this scan resolution, thus some interpretation of the images is required to classify the damage present. The predominant composite damage appears to be in the matrix; both intra-laminar cracks and delamination are seen. Looking through the thickness of the composite it is possible to identify the exact location of the change in fibre wind direction and thus distinguish between intra-laminar cracks and delamination (Figure 4). Close to the impact site there are damage features that are consistent with direct contact forces between the sample and the impactor. The damage features close to the surface are indicative of fibre breaks, evidenced by cracks crossing the direction of the fibres, in the external longitudinally wound layer (Figure 1). This is consistent with the study of Mitrevski *et al.* [7] who showed that sharper impactor shapes create more fibre breaks.

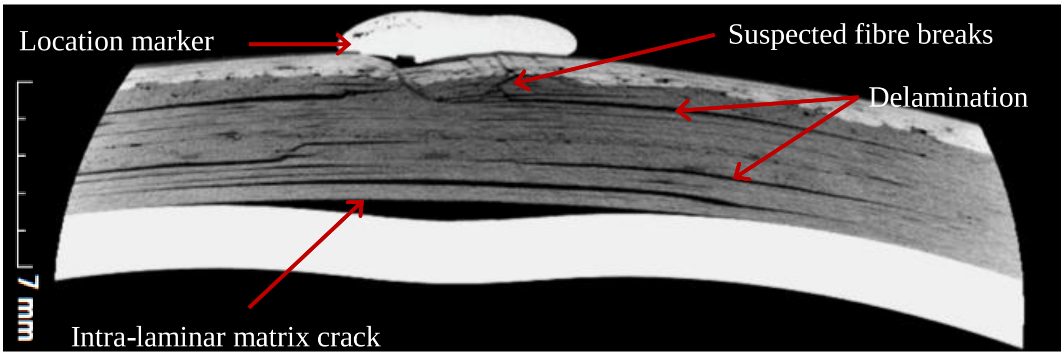

Figure 1: A single slice from the macro CT scan of the impact site perpendicular to the axis of the HCMS

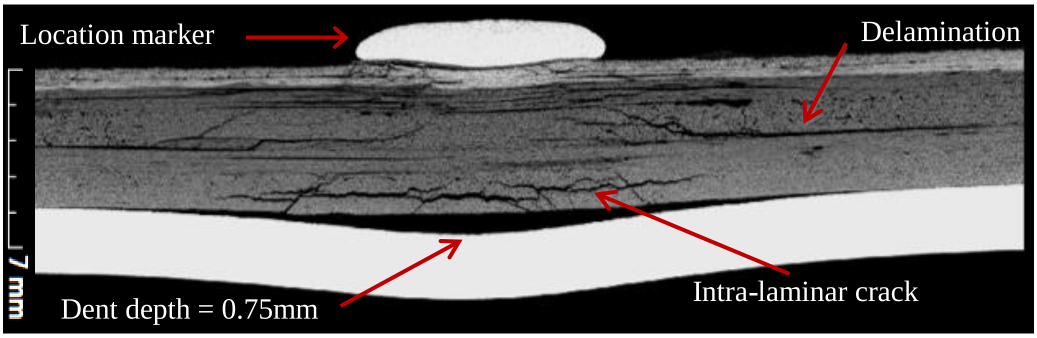

Figure 2: A single slice from the macro CT scan of the impact site in the long axis of the HCMS

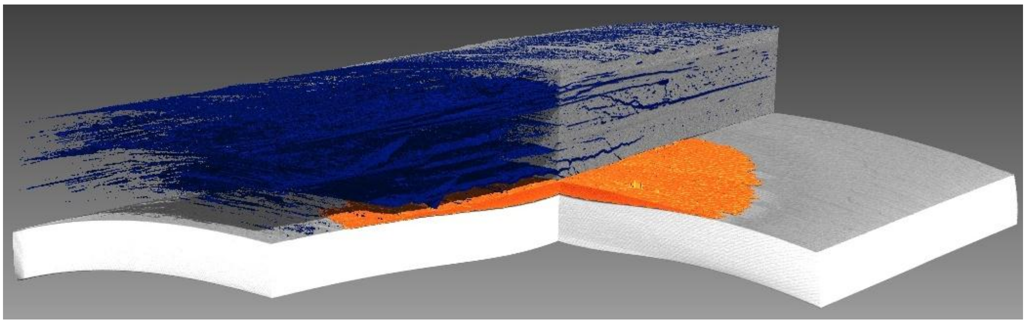

Figure 3 A 3D visualisation of the impact site with section cutouts. CFRP damage and voids are segmented in blue. The orange section is the dent in the metal layer

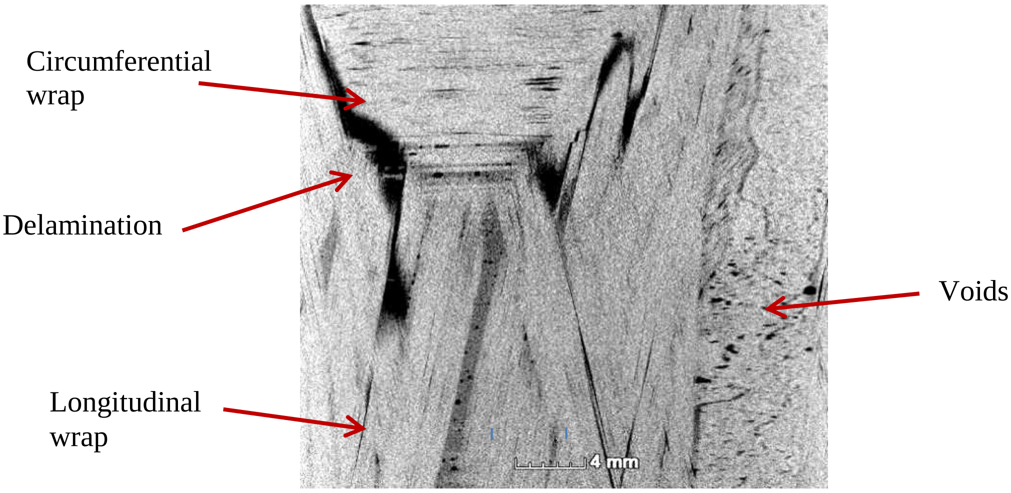

Figure 4: A slice through the thickness of the CFRP showing the change in wind direction

3.2 Meso-structure CT

A uniform load of 30MPa was applied to the sample. It was then prepared into matchstick samples at 0, 10mm and 20mm circumferentially from the centre of the impact site; a reference sample taken away from the impact site was also scanned. The scans presented in this section are at 10mm from the impact location and the reference sample.

3.2.1 Reference sample meso-structure scan

Scanning a reference sample from the same HCMS without the presence of impact damage enables quantification of the CFRP meso-structure. A 2D cross section of the reference matchstick sample reveals more detail as to the CFRP structure such as void content, void morphology and resin rich regions (Figure 5). Using the isosurface in-built tool in VGStudio max 2.1 the voids were segmented volumetrically and a void fraction, v_v, of ~3.5% was identified. At this resolution it is also possible to consider void morphology; two distinct geometries of voids are present in the CFRP (Figure 5). Long, thin voids that follow the fibre orientation within the plies are present in both the circumferential and longitudinally wrapped plies, forming in between fibres. More equi-axed, “globular” voids are also present; these have a tendency to occur either at ply boundaries or at the band overlap in the longitudinal layers. These locations are typically resin rich regions as highlighted in Figure 6.

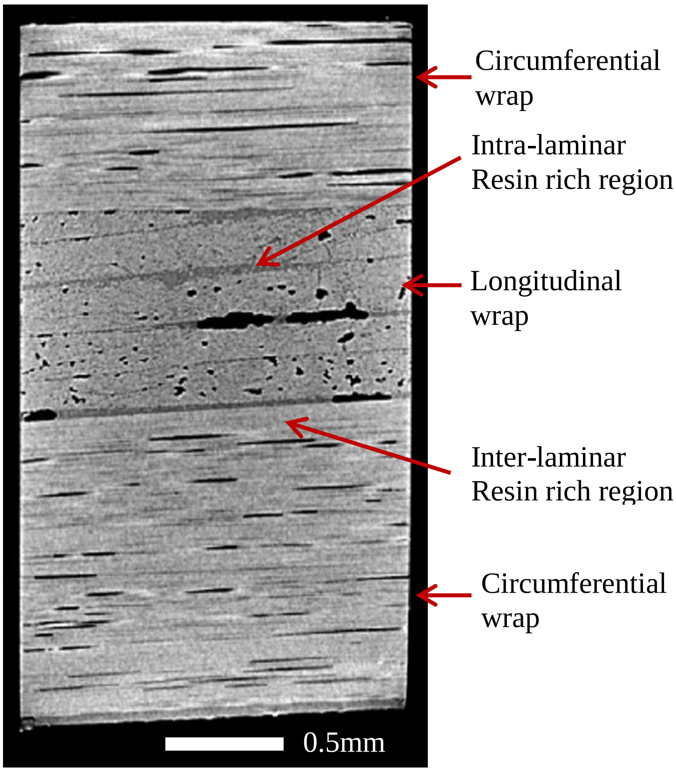

Figure 5: Unimpacted reference sample slice perpendicular to the axis of the sample

3.2.2 Impacted meso-structure scan

The higher resolution scans (4.6μm voxel size) give more fidelity of damage features that are not resolved at the 24μm resolution macroscopic impact site scans. Small intra-laminar cracks can be seen within the longitudinally wrapped ply (Figure 6B). At this length scale more detail of the crack path can be seen, showing multiple crack-void interactions. The ability to resolve more damage features shows that damage quantification at macro-scale impact site scales may not provide a complete picture of the material condition after impact. In these scans there is no evidence of fibre fracture within the material.

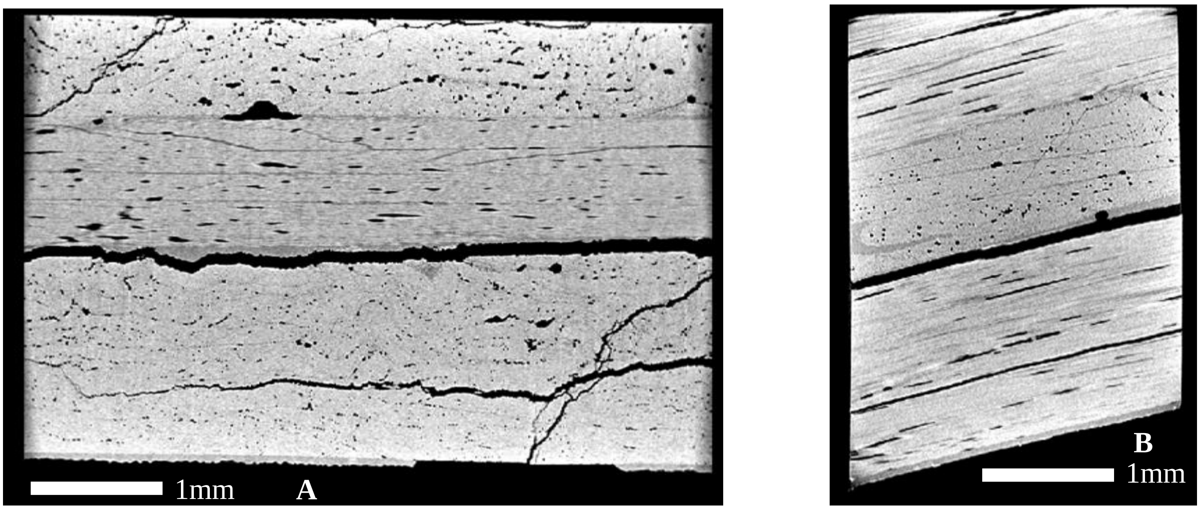

Figure 6: Longitudinal (A) and axial (B) view, 10mm from impact centre

3.3 Microstructure CT

The purpose of scanning at sub-micron resolutions is to investigate the presence of individual fibre breaks within the CFRP. With an imaged volume of ~1mm^3 per scan, covering an entire impact site with this technique is not a viable option. A series of scans covering ~4mm^3 were completed in the innermost circumferential wound layer directly under the impactor. This location was selected as it is the most likely place for fibre fracture to occur, as it is the location of the highest tensile load in the CFRP under the impact; no evidence of fibre breaks were present in the macro or mesoscopic scans in this location. Two cross sections in axial and longitudinal orientations are presented in Figure 7.

The presence of voids, of a similar size to a single fibre diameter, makes quantifying fibre breaks through automated segmentation tools difficult. Previous experience of the research group in assessing fibre breaks in similar resolution scans gives confidence in the ability to clearly distinguish between fibre breaks and micro voids due to the distinct morphology of fibre breaks [8, 9, 10]. Assessing all the scans generated, there is no evidence of individual fibre breaks within the CFRP in the scanned ROIs. As such, it is not expected that the tensile strength and stiffness of the circumferential CFRP layer have been significantly affected by the impact event and subsequent load cycle.

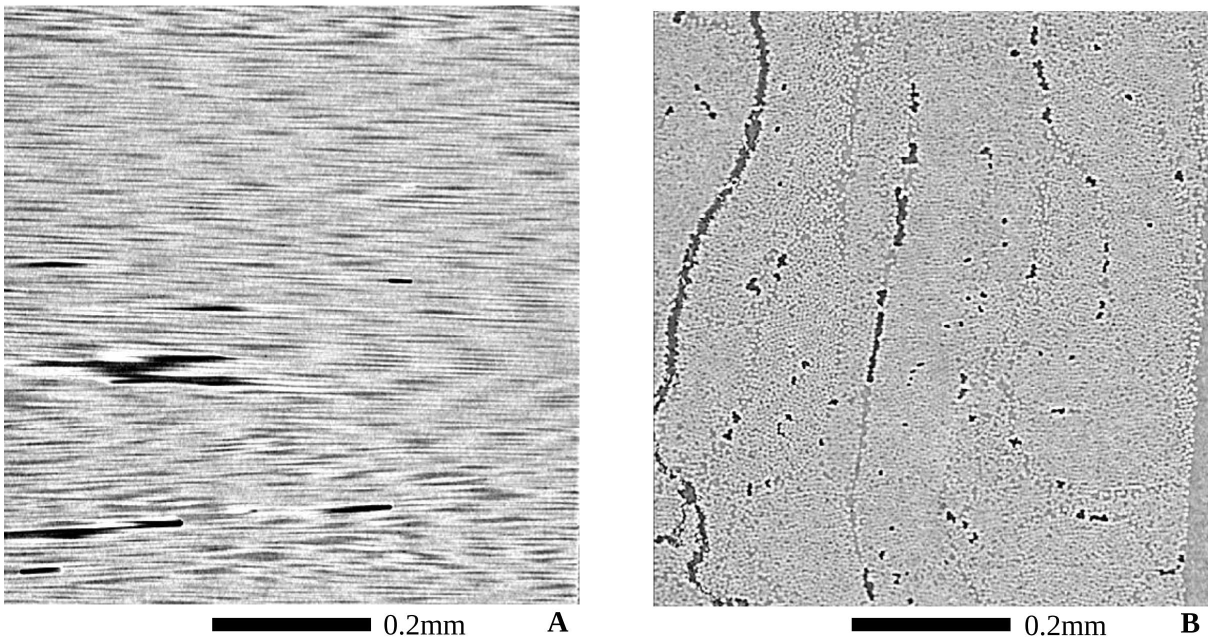

Figure 7: Longitudinal (A) and axial (B) views of micro-structure CT scans of ~1µm resolution at the inner-most circumferential wrapped ply.

4. Conclusions

The multi-scale imaging techniques used in the paper present a highly detailed view of the impact response of HCMS when impacted under an industrial LVI protocol. The impact response is a complex mix of: metal deformation, delamination, matrix cracks and suspected fibre breaks in the outer CFRP ply. Mesoscopic CT scans allowed for characterisation of the CFRP material structure, such as void volume fraction and gave more detail on crack paths through the CFRP. Microscopic scale CT results gave no evidence of isolated fibre breaks in the scanned ROIs directly under the impact location in the inner most circumferential layer, indicating that the strength and stiffness of circumferential wrapped CFRP is largely intact.

Acknowledgements
The authors would like to acknowledge the financial support of the EPSRC and Luxfer Gas Cylinders. Thanks also goes to Dr M Mavrogordato and Dr R Boardman for their help and expertise with the CT scanning completed in this work.

References

[1] Wakayama, S., Kobayashi, S., Imai, T., Matsumoto, T., *Evaluation of burst strength of FW-FRP composite pipes after impact using pitch-based low-modulus carbon fiber*. Composites Part A: Applied Science and Manufacturing, 2006. **37**(11): p. 2002-2010.

[2] Kobayashi, S., *Effect of autofrettage on durability of CFRP composite cylinders subjected to out-of-plane loading.* Composites Part B: Engineering, 2012. **43**(4): p. 1720-1726.

[3] Kobayashi, S., T. Imai, and S. Wakayama, *Burst strength evaluation of the FW-CFRP hybrid composite pipes considering plastic deformation of the liner.* Composites Part A: Applied Science and Manufacturing, 2007. **38**(5): p. 1344-1353.

[4] Kobayashi, S. and M. Kawahara, *Effects of stacking thickness on the damage behavior in CFRP composite cylinders subjected to out-of-plane loading.* Composites Part A: Applied Science and Manufacturing, 2012. **43**(1): p. 231-237

[5] Scott, A.E., Clinch, M., Hepples, W., Kalantzis, N., Sinclair, I., Spearing, S. M., *Advanced micro-mechanical analysis of highly loaded hybrid composite structures.* ICCM17: Procedings of the International Conference on Composite Materials, 27th - 31st July 2009, Edinburgh, UK.

[6] Bull, D.J., Spearing, S.M., Sinclair, I., Helfen, L., *Three-dimensional assessment of low velocity impact damage in particle toughened composite laminates using micro-focus X-ray computed tomography and synchrotron radiation laminography*. Composites Part A: Applied Science and Manufacturing, Volume 52, September 2013, p. 62-69.

[7] Mitrevski, T., Marshall, I.H., Thomson, R., *The influence of impactor shape on the damage to composite laminates.* Composite Structures, 2006. **76**(1–2): p. 116-122.

[8] Scott, A.E., Sinclair, I., Spearing, S.M., Mavrogordato, M.N., Hepples, W., *Influence of voids on damage mechanisms in carbon/epoxy composites determined via high resolution computed tomography*, Composites Science and Technology, 2014. **90**(10), p. 147-153

[9] Scott, A.E. Mavrogordato, M., Wright, P., Sinclair, I., Spearing, S.M. *In situ fibre fracture measurement in carbon–epoxy laminates using high resolution computed tomography*, Composites Science and Technology, 2011. **71**(12), p. 1471-1477

[10] Wright, P., Fu, X., Sinclair, I., Spearing, S.M., *Ultra high resolution computed tomography of damage in notched carbon fibre–epoxy composites,* Journal of Composite Materials, 2008. **48,** p. 1993–2002.